



REGULAR ARTICLE

Chemical Synthesis of  $ZnS_xSe_{1-x}$  Solid Solution Films from Aqueous Solutions Containing Sodium Hydroxide

M.A. Sozanskyi\* , R.R. Humnilovych, V.Ye. Stadnik, O.V. Klapchuk, P.Yo. Shapoval

Lviv Polytechnic National University, 79013 Lviv, Ukraine

(Received 28 September 2024; revised manuscript received 15 December 2024; published online 23 December 2024)

The zinc selenide-sulfide ( $ZnS_xSe_{1-x}$ ) films were synthesized on glass substrates by a chemical bath deposition. Aqueous solutions of zinc chloride, sodium hydroxide, hydrazine hydrate, thiourea and powdered elemental selenium were used for the preparation of working solutions. The thiourea and selenium concentrations were varied to obtain different substitutional parameter values ( $x$ ) of the films. The phase and elemental composition, optical transmittance spectra, and surface morphology of the deposited  $ZnS_xSe_{1-x}$  films were investigated. According to the X-ray diffraction analysis, the film samples were single-phase and consisted of the  $ZnS_xSe_{1-x}$  substitutionally solid solution in zincblende modification ( $ZnS$  structural type). The analysis of the elemental composition of the  $ZnS_xSe_{1-x}$  films showed that the  $x$  value changed from 0.11 to 0.85, depending on the variations in thiourea and selenium concentrations. The film's surface was solid and contained particles of spherical shape. The optical transmittance of the  $ZnS_xSe_{1-x}$  films increases across the investigated wavelength range from 340 to 900 nm. The transmittance curves have bends starting around the 340 nm region, shifting toward 650 nm for films with the highest selenium content, which is typical of  $ZnS_xSe_{1-x}$  solid solutions. The determined optical band gap values of the  $ZnS_xSe_{1-x}$  films ranged from 2.61 to 3.28 eV.

**Keywords:** Semiconductor films, Zinc sulfide, Zinc selenide, Solid Solution, Chemical deposition, XRD, Optical band gap.

DOI: [10.21272/jnep.16\(6\).06014](https://doi.org/10.21272/jnep.16(6).06014)

PACS numbers: 81.15.Lm, 78.66.Hf, 68.55.ag, 61.05.cp

1. INTRODUCTION

Zinc sulfide (ZnS) and zinc selenide (ZnSe) are wide-bandgap  $A^2B^6$  semiconductor materials with exceptional optical and electrical properties, making them attractive for various applications, including optoelectronics, photovoltaics, and photodetectors, etc.  $ZnS_xSe_{1-x}$ , an intermediate phase between ZnS and ZnSe, offers tunable bandgap energy, which can be modulated by adjusting the sulfur (S) and selenium (Se) content in the film. This tunability enhances its potential for specific device applications such as light-emitting diodes (LEDs), lasers, and solar cells, where precise control over the optical absorption and emission spectra is crucial.

Among the various methods for producing  $ZnS_xSe_{1-x}$  films, chemical deposition techniques such as chemical bath deposition (CBD) [1, 2], chemical surface deposition (CSD) [2, 3], and successive ionic layer adsorption and reaction (SILAR) [4, 5], have gained attention due to their simplicity, low cost, and ability to deposit films over large areas and substrates. These methods offer advantages in terms of scalability, and control over the film's composition, structure, bandgap, etc. Additionally, they can be carried out at low temperatures, which is crucial for depositing films on temperature-sensitive substrates, such as those used in flexible electronics.

This study focuses on the CBD of  $ZnS_xSe_{1-x}$  films and examines the effect of various ratio of chalcogeniz-

ers on the structural, optical, and morphological properties of  $ZnS_xSe_{1-x}$  films. The method of deposition used in this work allows control over the films' S : Se ratio, making it possible to systematically investigate the relationship between composition and material properties. By tuning the appropriate deposition conditions, we aim to optimize films for potential applications in optoelectronics and related technologies.

2. EXPERIMENTAL DETAILS

2.1 Materials

To obtain  $ZnS_xSe_{1-x}$  films, we used the following chemical reagents: zinc chloride ( $ZnCl_2$ ), sodium hydroxide (NaOH), hydrazine hydrate ( $N_2H_4 \cdot H_2O$ ), thiourea ( $(NH_2)_2CS$ ) and elemental powdered selenium (Se), which was dissolved in the alkaline  $N_2H_4 \cdot H_2O$  solution. Glass plates were used as the substrate material with unit dimensions of 24 mm  $\times$  24 mm.

2.2 Methods

The  $ZnS_xSe_{1-x}$  films were synthesized from prepared working solutions using the CBD method. To achieve this, appropriate quantities of  $ZnCl_2$  and NaOH were dissolved in distilled water, mixed, then transferred into a bath, and heated to form the soluble tetrahydroxozincate(II) complex  $[Zn(OH)_4]^{2-}$ . Following

\* Correspondence e-mail: [martyn.a.sozanskyi@lpnu.ua](mailto:martyn.a.sozanskyi@lpnu.ua)



this, to initiate the film deposition,  $(\text{NH}_2)_2\text{CS}$  and Se solutions were added, and glass substrates were placed into the bath. The molar concentrations of the components in the working solutions, as well as the deposition duration and temperature, are provided in Table 1. Once the deposition process was complete, the substrates were removed from the bath, cleaned with distilled water, and air-dried. The installation scheme used for obtaining  $\text{ZnS}_x\text{Se}_{1-x}$  films by the CBD method is shown in Fig. 1, and the synthesized  $\text{ZnS}_x\text{Se}_{1-x}$  films are presented in Fig. 2.

**Table 1** – The conditions for the  $\text{ZnS}_x\text{Se}_{1-x}$  films deposition

Index	Value				
C( $\text{ZnCl}_2$ ), mol/L	0.08				
C( $\text{NaOH}$ ), mol/L	5.0				
C( $\text{N}_2\text{H}_4 \cdot \text{H}_2\text{O}$ ), mol/L	0.15				
C(Se), mol/L	0.09	0.07	0.05	0.03	0.01
C( $(\text{NH}_2)_2\text{CS}$ ), mol/L	0.01	0.03	0.05	0.07	0.09
Se : $(\text{NH}_2)_2\text{CS}$ molar ratio	9 : 1	7 : 3	5 : 5 (1 : 1)	3 : 7	1 : 9
Volume of working solution, mL	200				
Process duration, min	40				
pH of working solution	~ 14				
Temperature, °C	70				

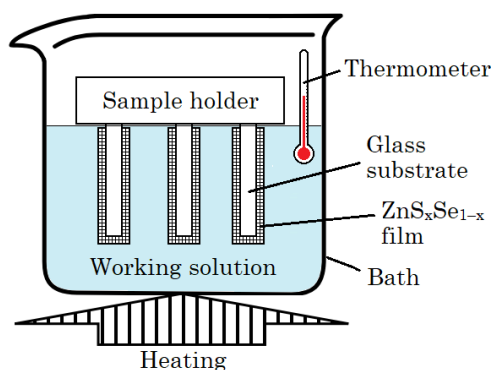


**Fig. 1** – The installation scheme used for obtaining  $\text{ZnS}_x\text{Se}_{1-x}$  films by the CBD method

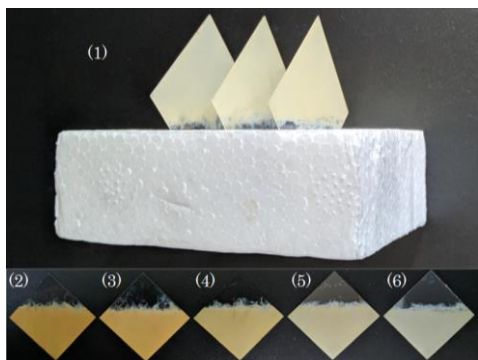


**Fig. 2** – A sample holder with the synthesized film samples (1) and a row of the  $\text{ZnS}_x\text{Se}_{1-x}$  films synthesized with various Se :  $(\text{NH}_2)_2\text{CS}$  molar ratios: 9 : 1 (2); 7 : 3 (3); 5 : 5 (1 : 1) (4); 3 : 7 (5), and 1 : 9 (6)

X-ray diffraction patterns (XRD, diffractograms) of the  $\text{ZnS}_x\text{Se}_{1-x}$  films were obtained using an Aeris Research X-ray diffractometer ( $\text{CuK}\alpha^-$  radiation) over a

$2\theta$  angle range of 10-100 degrees, with a step size of 0.01 degree. Phase identification from the experimental diffractograms was performed using the PowderCell program [6].

Elemental analysis of the  $\text{ZnS}_x\text{Se}_{1-x}$  films to determine the molar (atomic) ratio of Zn, S, and Se was carried out using an X-ray fluorescence (XRF) spectrometer, ElvaX Light SDD (Elvatech).

The optical transmittance spectra,  $T(\lambda)$ , of the  $\text{ZnS}_x\text{Se}_{1-x}$  films were measured over a wavelength range ( $\lambda$ ) of 340-900 nm using a Xion 500 spectrophotometer, with a measurement accuracy of  $\pm 0.5\%$ . To determine the optical bandgaps ( $E_g$ ) of the deposited  $\text{ZnS}_x\text{Se}_{1-x}$  films, the Tauc method was employed, as shown in [7].

Surface morphology images of the  $\text{ZnS}_x\text{Se}_{1-x}$  films were captured on a REMMA-102-02 scanning electron microscope (SEM). Additionally, to obtain focused SEM images, it was necessary to sputter a thin carbon layer onto the surface of the films.

### 3. RESULTS AND DISCUSSION

#### 3.1 Structural Properties and Elemental Analysis

XRD analysis was performed on the  $\text{ZnS}_x\text{Se}_{1-x}$  films. As shown in Fig. 3, the diffractograms display a dominant peak in the  $27.5\text{-}28.5^\circ$  range, along with two weaker peaks at  $45.8\text{-}47.6^\circ$  and  $54.5\text{-}56.3^\circ$ . These peaks correspond to the (111), (220), and (311) planes of the cubic zincblende phase ( $\text{ZnS}$  structural type). They are located between the theoretical diffraction lines of  $\text{ZnS}$  and  $\text{ZnSe}$  compounds, which is characteristic of the intermediate phase between these compounds, i.e. the  $\text{ZnS}_x\text{Se}_{1-x}$  substitutional solid solution.

Elemental analysis of the obtained film samples by XRF was made. The selected elements for determination were Zn, S, and Se, as other detected elements belong to the glass substrate. The results (Fig. 4) showed that varying the concentrations of selenium and thiourea led to a molar (atomic) ratio of Zn : S : Se in the films ranging from 1 : 0.11 : 0.89 to 1 : 0.85 : 0.15, respectively. This corresponds to a change in the substitutional parameter ( $x$ ) from 0.11 to 0.85 in the  $\text{ZnS}_x\text{Se}_{1-x}$  solid solution.

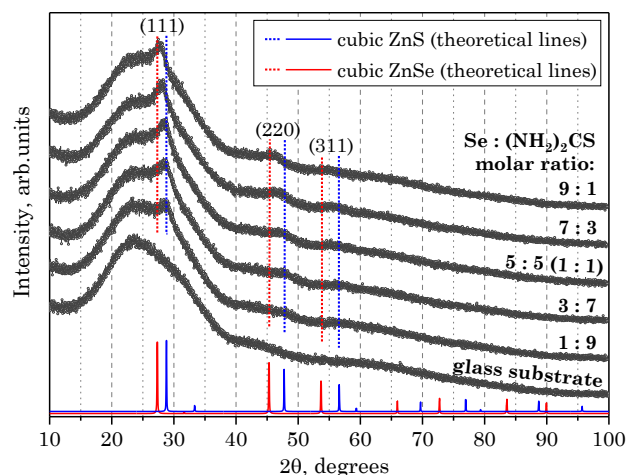


**Fig. 3** – XRD patterns of the obtained  $\text{ZnS}_x\text{Se}_{1-x}$  films on glass substrates and a XRD pattern of the clean glass substrate for comparison

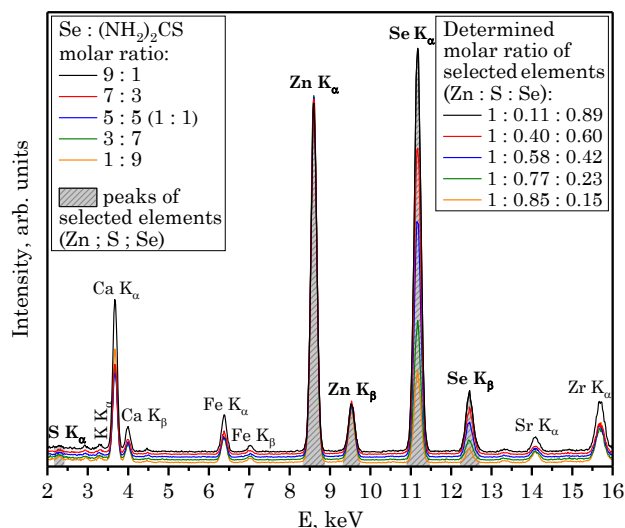


**Fig. 4** – XRF spectra of the obtained  $ZnS_xSe_{1-x}$  films on glass substrates and the results of Zn, S, and Se element determination

### 3.2 Morphological Properties

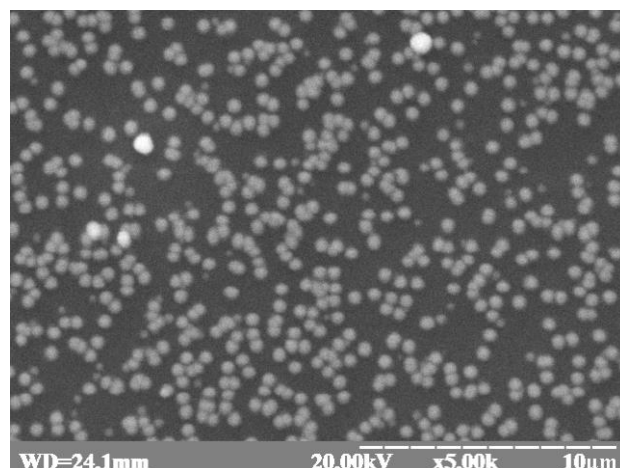
The results of the surface morphology investigation of the  $ZnS_xSe_{1-x}$  film samples are shown in Fig. 5. The microphotographs indicate that the  $ZnS_xSe_{1-x}$  films surface is solid and contains particles of a spherical shape. The varying concentrations of thiourea and selenium does not significantly effect on the films surface morphology. The similar picture of spherical particles we also observed earlier on the surface of synthesized ZnS and ZnSe films [8, 9] from sodium hydroxide solutions as well as other authors [10-13]. This may be due to the viscosity of the working solution caused by NaOH.

### 3.3 Optical Properties

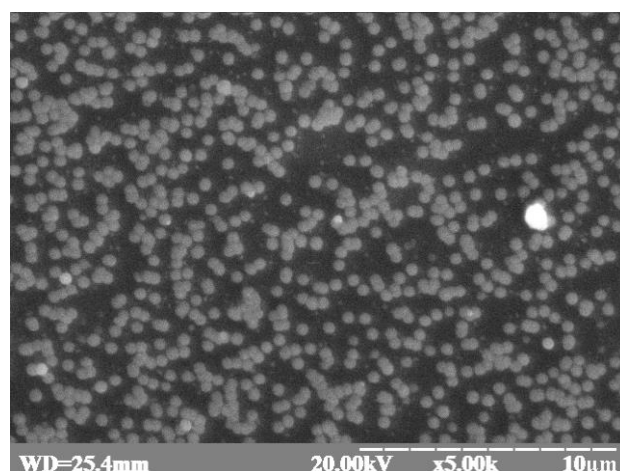
The optical transmission spectra  $T(\lambda)$  of the  $ZnS_xSe_{1-x}$  films synthesized with various molar ratios of Se :  $(NH_2)_2CS$  were recorded (Fig. 6). The transmittance ( $T$ ) increases over the entire measured wavelength range (340-900 nm). Prominent bends or sharper rises in the transmittance curves are observed between approximately 340 and 650 nm, with these features shifting toward longer wavelengths as the Se content in the  $ZnS_xSe_{1-x}$  films increases in response to changes in the Se :  $(NH_2)_2CS$  molar ratio. Such bends in the  $T(\lambda)$  curves are typical of  $A^2B^6$  semiconductor films and depend on the specific chalcogenide compound from the zinc subgroup [10-12, 14-16]. As for  $ZnS_xSe_{1-x}$  films, which contain both chalcogenides, their  $T(\lambda)$  spectra (Fig. 6) have an intermediate form [17] between the two corresponding binary chalcogenides, ZnS [8] and ZnSe [9].

The optical bandgaps ( $E_g$ ) of the  $ZnS_xSe_{1-x}$  films were determined (Fig. 7). The  $E_g$  values decreased as the Se content increased in the deposited  $ZnS_xSe_{1-x}$  films. For instance, the  $ZnS_xSe_{1-x}$  film with an S : Se atomic ratio of 0.85 : 0.15 shows an  $E_g$  of 3.28 eV. The rest of the optical bandgap values were found to be 3.05 eV, 2.98 eV, 2.83 eV, and 2.61 eV, corresponding to the previously determined S : Se atomic ratios of

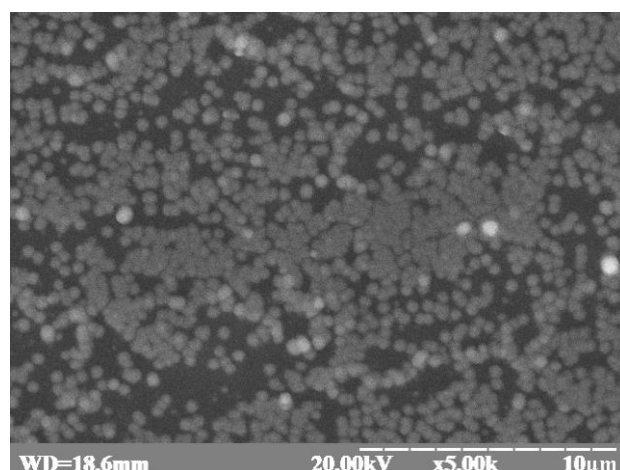
0.77 : 0.23, 0.58 : 0.42, 0.40 : 0.60, and 0.11 : 0.89 in the  $ZnS_xSe_{1-x}$  films composition (Fig. 4), respectively.



a



b



c

**Fig. 5** – SEM images ( $\times 5000$  magnification) of surface morphology of the  $ZnS_xSe_{1-x}$  films synthesized with Se :  $(NH_2)_2CS$  molar ratios: 9 : 1 (a); 5 : 5 (1 : 1) (b), and 1 : 9 (c)

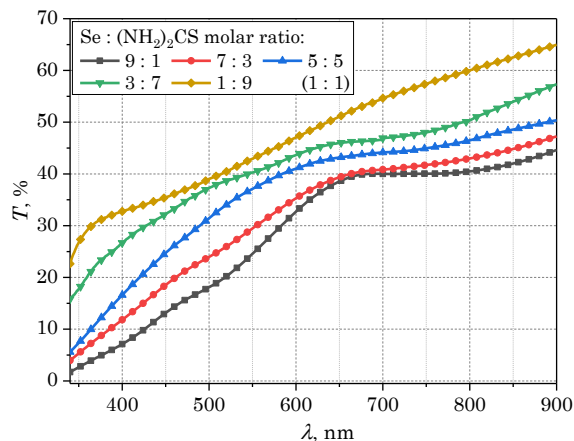


Fig. 6 – Optical transmittance spectra of the  $\text{ZnS}_x\text{Se}_{1-x}$  films

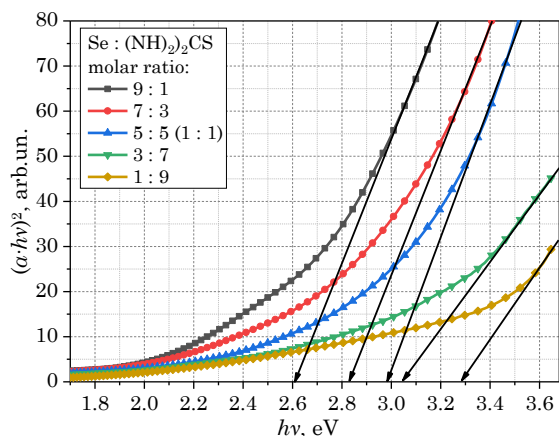


Fig. 7 –  $(\alpha \cdot hv)^2 = f(hv)$  dependences and determination of the optical bandgap values of the  $\text{ZnS}_x\text{Se}_{1-x}$  films

## REFERENCES

- S.M. Pawar, B.S. Pawar, J.H. Kim, O.S. Joo, C.D. Lokhande, *Curr. Appl. Phys.* **11**, 117 (2011).
- M.A. Sozanskyi, P.Yo. Shapoval, T.B. Gnativ, R.R. Guminilovych, V.E. Stadnik, M.M. Laruk, *J. Nano-Electron. Phys.* **14** No 5, 05026 (2022).
- P. Shapoval, R. Guminilovych, I. Yatchyshyn, *Chem. Chem. Technol.* **7** No 3, 345 (2013).
- B. Benmazouza, T. Sahraoui, M. Adnane, N. Hamamousse, A. Djelloul, Y. Larbah, L. Benharrat, *J. Nano-Electron. Phys.* **15** No 2, 02010 (2023).
- J.O. Sigala-Valdez, O.Y. Ramirez-Ezquivel, C.L. Castañeda-Miranda, H. Moreno-García, R. García-Rocha, I.L. Escalante-García, A. Del Rio-De Santiago, *Heliyon* **9** No 7, e17971 (2023).
- T. Roisnel, J. Rodríguez-Carvajal, *Mater. Sci. Forum* **378-381**, 118 (2001).
- A.V. Raval, I.A. Shaikh, V.M. Jain, N.M. Shastri, P.B. Patel, L.K. Saini, D.V. Shah, *J. Nano-Electron. Phys.* **12** No 2, 02010 (2020).
- P. Shapova, M. Sozanskyi, I. Yatchyshyn, B. Kulyk, M. Shpotyuk, R. Gladyshevskii, *Chem. Chem. Technol.* **10** No 3, 317 (2016).
- M.A. Sozanskyi, P.Y. Shapoval, R.T. Chaykivska, V.E. Stadnik, Y.Y. Yatchyshyn, *Bulletin of the Lviv Polytechnic National University. Series of Chemistry, Materials Technology and Their Application* **841** No 16, 36 (2016).
- H.K. Sadekar, N.G. Deshpande, Y.G. Gudage, A. Ghosh, S.D. Chavhan, S.R. Gosavi, R. Sharma, *J. Alloy. Compd.* **453** No 1-2, 519 (2008).
- I.J. González-Chan, A. Pat-Herrera, A.I. Trejo-Ramos, A.I. Oliva, *Surf. Eng.* **37** No 9, 1120 (2021).
- D.S. Sofronov, O.M. Sofronova, E.I. Kostenyukova, V.V. Starikov, A.M. Lebedinskiy, P.V. Mateychenko, A.S. Opanasyuk, *J. Nano-Electron. Phys.* **6** No 1, 01016 (2014).
- D.S. Sofronov, E.A. Vaksler, P.V. Mateychenko, O.M. Sofronova, A.M. Lebedynskiy, V.V. Starikov, E.A. Samoilo, *J. Nano-Electron. Phys.* **9** No 3, 03009 (2017).
- R. Kulkarni, A. Pawbake, R. Waykar, A. Jadhawar, H. Borate, R. Aher, A. Bhorde, S. Nair, P. Sharma, S. Jadar, *J. Nano-Electron. Phys.* **10** No 3, 03005 (2018).
- M.A. Sozanskyi, K.M. Siryk, P.Yo. Shapoval, R.R. Huminirovych, V.E. Stadnik, M.M. Laruk, *J. Nano-Electron. Phys.* **15** No 6, 06010 (2023).
- M. Sozanskyi, V. Stadnik, P. Shapoval, I. Yatchyshyn, R. Guminilovych, S. Shapoval, *Chem. Chem. Technol.* **14** No 3, 290 (2020).
- V.S. Ganesha Krishna, M.G. Mahesha, *Surf. Interfaces* **20**, 100509 (2020).
- K. Dashtian, N. Shahbazi, F. Amourizi, B. Saboorizadeh, A. Mousavi, S.S. Astaraei, R. Zare-Dorabei, *Fundamentals of Sensor Technology: Principles and Novel Designs*, 551 (Elsevier – Woodhead Publishing: 2023).

## 4. CONCLUSIONS

The  $\text{ZnS}_x\text{Se}_{1-x}$  films were synthesized on glass substrates via the chemical bath deposition technique using different molar ratios of chalcogenizers. The resulting films were confirmed to be single-phase and consist of an intermediate  $\text{ZnS}_x\text{Se}_{1-x}$  composition between ZnS and ZnSe. Optical transmittance spectra of the  $\text{ZnS}_x\text{Se}_{1-x}$  films were analysed, and the optical bandgap values were found to vary within the range of 2.61 to 3.28 eV, corresponding to the variations of S : Se atomic ratio in the films. Their surface was solid and contained spherical-shaped particles.

The findings from this study suggest that  $\text{ZnS}_x\text{Se}_{1-x}$  films, as a mixed  $\text{A}^2\text{B}^6$  semiconductor material, show promise for further exploration and potential use in semiconductor devices for various electronic applications [18].

## ACKNOWLEDGMENTS

This work was carried out with the support of the Ministry of Education and Science of Ukraine as part of the scientific work of the project for young scientists «Theoretical and Experimental Bases of Chemical Synthesis of Modified  $\text{A}^2\text{B}^6$ -type Film Semiconductors for Alternative Energy» (state registration number 0124U000522).

The analysis of the film samples was performed using the equipment of the Centre of Collective Use of Scientific Equipment: the «Laboratory of Perspective Technologies, Creation and Physico-Chemical Analysis of New Substances and Functional Materials» at the Lviv Polytechnic National University (<https://lpnu.ua/ckkno>).

**Хімічний синтез плівок твердого розчину  $ZnS_xSe_{1-x}$  з водних розчинів, що містять гідроксид натрію**

М.А. Созанський, Р.Р. Гумінілович, В.Є. Стаднік, О.В. Клапчук, П.Й. Шаповал

*Національний університет «Львівська політехніка», 79013 Львів, Україна*

Плівки селеніду-сульфіду цинку ( $ZnS_xSe_{1-x}$ ) були синтезовані на скляних підкладках шляхом хімічного осадження у ванні. Для приготування робочих розчинів використовували водні розчини цинк хлориду, натрію гідроксиду, гідразин гідрату, тіосечовини та порошкоподібного елементарного селену. Концентрації тіосечовини та селену змінювали для отримання різних значень параметра заміщення ( $x$ ) плівок. Досліджено фазовий та елементний склад, спектри оптичного пропускання та морфологію поверхні осаджених плівок  $ZnS_xSe_{1-x}$ . За даними рентгенодифракційного аналізу зразки плівок були однофазними і склалися з твердого розчину заміщення  $ZnS_xSe_{1-x}$  у модифікації цинкової обманки (структурний тип ZnS). Аналіз елементного складу плівок  $ZnS_xSe_{1-x}$  показав, що величина  $x$  змінювалася від 0,11 до 0,85 залежно від зміни концентрацій тіосечовини та селену. Поверхня плівки була твердою і містила частинки сферичної форми. Оптичне пропускання плівок  $ZnS_xSe_{1-x}$  зростає в досліджуваному діапазоні довжин хвиль від 340 до 900 нм. Криві пропускання мають вигини, починаючи з області 340 нм, зсуваючись до 650 нм для плівок з найвищим вмістом селену, що характерно для твердих розчинів  $ZnS_xSe_{1-x}$ . Визначені оптичні значення ширини забороненої зони плівок  $ZnS_xSe_{1-x}$  становили від 2,61 до 3,28 eV.

**Ключові слова:** Напівпровідникові плівки, Сульфід цинку, Селенід цинку, Твердий розчин, Хімічне осадження, XRD, Оптична ширина забороненої зони.